I.UZUN

USE OF PORE SCALE SIMULATORS TO UNDERSTAND THE EFFECTS OF WETTABILITY ON MISCIBLE CARBON DIOXIDE FLOODING AND INJECTIVITY

ILKAY UZUN

DECEMBER 2005

METU 2005

USE OF PORE SCALE SIMULATORS TO UNDERSTAND THE EFFECTS OF WETTABILITY ON MISCIBLE CARBON DIOXIDE FLOODING AND INJECTIVITY

A THESIS SUBMITTED TO
THE GRADUATE SCHOOL OF NATURAL AND APPLIED SCIENCES
OF
MIDDLE EAST TECHNICAL UNIVERSITY

BY

ILKAY UZUN

IN PARTIAL FULFILLMENT OF THE REQUIREMENTS
FOR
THE DEGREE OF MASTER OF SCIENCE
IN
PETROLEUM AND NATURAL GAS ENGINEERING

Approval of the Graduate School of Natural and Applied Sciences

Prof. Dr. Canan Özgen
Director

I certify that this thesis satisfies all the requirements as a thesis for the degree of Master of Science.

Prof.Dr. Birol Demiral
Head of Department

This is to certify that we have read this thesis and that in our opinion it is fully adequate, in scope and quality, as a thesis for the degree of Master of Science

Assoc. Prof.Dr. Serhat Akin
Supervisor

Examining Committee Members

Prof. Dr. Birol Demiral	(METU,PETE)	_____
Assoc. Prof.Dr. Serhat Akin	(METU,PETE)	_____
Prof.Dr. Mahmut Parlaktuna	(METU,PETE)	_____
Prof.Dr. Mustafa V. Kök	(METU,PETE)	_____
Ugur Karabakal (MSc.)	(TPAO)	_____

I hereby declare that all information in this document has been obtained and presented in accordance with academic rules and ethical conduct. I also declare that, as required by these rules and conduct, I have fully cited and referenced all material and results that are not original to this work.

Name, Last name :ILKAY UZUN

Signature:

ABSTRACT

USE OF PORE SCALE SIMULATORS TO UNDERSTAND THE EFFECTS OF WETTABILITY ON MISCIBLE CARBON DIOXIDE FLOODING AND INJECTIVITY

Uzun, Ilkay

M.Sc., Department of Petroleum and Natural Gas Engineering

Supervisor: Assoc.Prof. Dr. Serhat AKIN

December 2005, 63 pages

This study concentrates on the modelling of three phase flow and miscible CO_2 flooding in pore networks that captures the natural porous medium of a reservoir. That is to say, the network, that is a Matlab code, consists of different sided triangles which are located randomly through the grids. The throats that connect the pores are also created by the model. Hence, the lengths and the radii of the throats are varying. The network used in this research is assumed to be representative of mixed-wet carbonates in 2-D. Mixed wettability arises in real porous media when oil renders surfaces it comes into prolonged contact with oil-wet while water-filled nooks and crannies remain water-wet. The model developed is quasi-static approach to simulate two phase and three phase flows. By this, capillary pressures, relative permeabilities, saturations, flow paths are determined for primary drainage, secondary imbibition, and CO_2 injection cases. To calculate the relative permeability, capillary entry pressures are first determined. Then, hydraulic conductances and flow rates of the network for each grid are obtained. Phase

areas and saturations are also determined. It is accepted that the displacement mechanism in drainage and CO_2 injection is piston-like whereas in imbibition it is either piston-like or snap-off.

The results of the model are compared with the experimental data from the literature. Although, the pore size distribution and the contact angle of the model are inconsistent with the experimental data, the agreement of the relative permeabilities is promising.

The effect of contact angle in the same network for three phase flow where immiscible CO_2 is injected as a third phase at supercritical temperature (32 °C) is investigated. And it is found that, the increase in the intrinsic angles causes decrease in relative permeability values.

As another scenario, two phase model is developed in which miscible CO_2 – water is flooded after the primary drainage of the same 2-D network at supercritical temperature (32 °C). This case is compared with the previous case and the effects of miscibility are investigated such that it causes the relative permeability values to increase.

Adsorption is another concern of which its effects are analyzed in a single pore model. The model is compared with the reported experimental data at high temperature and pressures. A reasonable fit is obtained.

Keywords: Pore Networks, Three Phase Relative Permeability, CO_2, Miscibility, Wettability, Adsorption

ÖZ

GÖZENEK ÖLÇEKLI SIMULATÖRLERIN KULLANIMIYLA ISLATIMLILIGIN, KARISABILIR KARBON DIOKSIT ÖTELEMESI VE ENJEKSIYONU ÜZERINDEKI ETKILERININ ANLASILMASI

Uzun, Ilkay
Y.Lisans, Petrol ve Dogal Gaz Mühendisligi Bölümü
Tez Yöneticisi: Doç. Dr. Serhat Akin

Aralik 2005, 63 sayfa

Bu çalisma, rezervuardaki dogal gözenek ortamini yakalayan gözenekli aglarda üç fazli akis ve karisabilir CO_2 ötelemesinin modellenmesi üzerine yogunlastirilmistir. Matlab ile kodlanmis olan ag, hatlar içinde rastgele yerlestirilmis farkli kenarli üçgenlerden olusmaktadir. Gözenekleri birbirine baglayan gözenek bogazlari da model tarafindan olusturulmaktadir. Böylece, geçitlerin uzunluklari ve yariçaplari degiskendir. Bu çalismada kullanilan agin iki boyutlu karisik islatimli karbonatlari temsil ettigi farzedilmektedir. Gerçek gözenek ortamlarinda karisik islatimlilik, petrolün yüzeyi erirken uzun süre petrol islatimiyla temas etmesi bu arada su ile dolmus köse ve çatlaklarin su islatimli kalmasi ile ortaya çikar. Gelistirilen model, iki fazli ve üç fazli akislarin simulasyonunu yapan quasi-statik yaklasimdir. Böylece, kilcal basinçlar, göreli geçirgenlik, doymusluklar ve akis yolu birincil drenaj, su ötelemesi ve CO_2 enjeksiyonu durumlari için elde edilmistir. Göreli geçirgenlikleri hesaplamak için ilk önce kilcal esik basinçlari tayin edilmistir. Daha sonra agdaki herbir hat için hidrolik iletkenlikler ve akis hizlari bulunmustur. Bundan baska, faz alanlari ve doygmusluklar

tayin edilmistir.Drenaj ve CO_2 ötelemesinde piston-tipi, su ötelenmesinde ise piston-tipi veya kopma gözenek düzeyinde yerdegisim mekanizmalari olarak kullanilmistir.

Modelin sonuçlari, literatürde bulunan deneysel verilerle karsilastirilmistir. Modelin gözenek boyut dagilimi ve degme açisi deneysel verilerden farkli olmasina ragmen göreli geçirgenligin uyumu umut vericidir.

Süper kritik sicaklikta (32 °C) üçüncü bir faz olan karismaz CO_2 ötelemesi ile üç fazli akisin ayni agda temas açisi etkileri incelenmistir ve gerçel açilardaki artisin göreceli geçirgenlik degerlerinin azalmasina neden oldugunu bulunmustur.

Diger bir senaryo ise, karisabilir CO_2 – suyun birincil drenajdan sonra ayni iki boyutlu agdan süper kriritik sicaklikta (32 °C) ötelemesi ile iki boyutlu model gelistirilmesidir. Bu durum, bir önceki durumla karsilastirilmis ve karisabilirligin göreli geçirgenlik degerlerini artirmasi gibi sonuçlar elde edilmistir.

Sogurulma, tek gözenekli bir modelde etkileri arastirilan diger bir faktördür. Model, yazili deneysel verilerle yüksesk sicaklik ve basinçta karsilastirilmistir. Kabul edilebilir uygunluk elde edilmistir.

Anahtar Kelimeler: Gözenek agi, Üç-Fazli Göreceli Geçirgenlik, CO_2, Karisabilirlik, Islatimlilik, Sogurma

To My Parents and Brother

ACKNOWLEDGMENTS

I would like to thank my advisor Assoc.Prof.Dr. Serhat Akin for his constant support, guidance and encouragement during this study. Without his assistance, this work would have not been accomplished. My thesis committee Prof. Dr. Birol Demiral, Assoc. Prof. Dr. Serhat Akin, Prof. Dr. Mahmut Parlaktuna, Prof.Dr. Mustafa V. Kök, Ugur Karabakal are very appreciated for their comments and suggestions.

Finally my special thanks go to my family and my friends Suphi Çeviker, Çigdem Ömürlü and Erdinç Eker. With their prayers, supports, encouragements and considerations this thesis became a reality.

TABLE OF CONTENTS

LIST OF TABLES

LIST OF FIGURES

CHAPTER 1
INTRODUCTION

Pore-scale network models provide a unique computational bridge between the pore and continuum scales. A simulated network of pores as a computational system within which pore-scale physical processes are modelled. The pore networks are used mainly to describe the macroscopic properties such as relative permeability (Dixit et al., 1997), capillary pressures (Jerauld and Salter, 1990), and electrical properties (Oren and Bakke, 2002). The macroscopic descriptors of multiphase flow of fluids, such as relative permeabilities and capillary pressures, are the volume-averaged continuum functions with origin in the displacement mechanism at the microscopic or pore scale (Bear, 1972). Therefore, these functions can be predicted if there is an adequate description of essential geometry and topology of the pore space, and a representation of the multiphase flow physics (Al-Futaisi, 2002). Pore networks are also used in fractured reservoirs in single, two or three phase flows (Chatzis and Dullien, 1977; Bakke and Oren 1997).

The macroscopic transport properties of two phase flow are determined not only by the geometry and topology of the porous medium, but also by the spatial distribution of wettability and the extent of wettability alteration in individual pores (Al-Futaisi, 2002). Several studies have used pore network models to investigate the effect of wettability on the macroscopic descriptors of two phase flow (Blunt, 1997a; Blunt, 1997b; Heiba et al., 1983; McDougall and Sorbie, 1995).

Pore networks are used to simulate the reservoir since they are representatives of reservoirs where conducting experiments are expensive; time consuming and even not possible, for instance, experiments at supercritical temperature of CO_2 is very difficult.

In this study, a pore network model to study CO_2 injection at supercritical temperature (32 °C) is studied that has gone through primary drainage, secondary imbibition. This thesis is organized as follows. In Chapter 2, literature overview is briefly described. In Chapter 3, the physics of two and three phase flows in a single pore is described, i.e., the theory for calculating capillary entry pressure, phase areas, saturations, hydraulic conductances, flow rates and relative permeabilities are described. In Chapter 4, statement of the problem is presented. In Chapter 5, the results are shown. The simulator is validated against experiments and for other cases, simulator is run, i.e., the cases for immiscible and miscible CO_2 at supercritical temperature (32 °C). Finally, in Chapter 6, the thesis is concluded with the most important findings and accomplishments of this research.

CHAPTER 2
LITERATURE OVERVIEW

Pore network modelling is a technique to model multiphase flow at the small scale and to predict average macroscopic properties, such as permeability, capillary pressure, relative permeability and residual oil saturation. Traditionally, network models represented the void space of a rock by a regular two- or three-dimensional lattice of wide pores connected by narrower throats. Each pore or throat is assumed to be cylindrical, triangular or spherical (Figure1) and hence contain just one phase. The coordination number (the number of throats connected to a pore) can vary depending on the chosen lattice. In order to match the coordination number of a given rock sample, which typically is between 3 and 8 (Jerauld and Salter, 1990), it is possible to remove throats from a lattice of higher coordination number. To better reflect real porous media it is possible to randomly distribute points within the model area and then construct a network from the triangulation of these points.

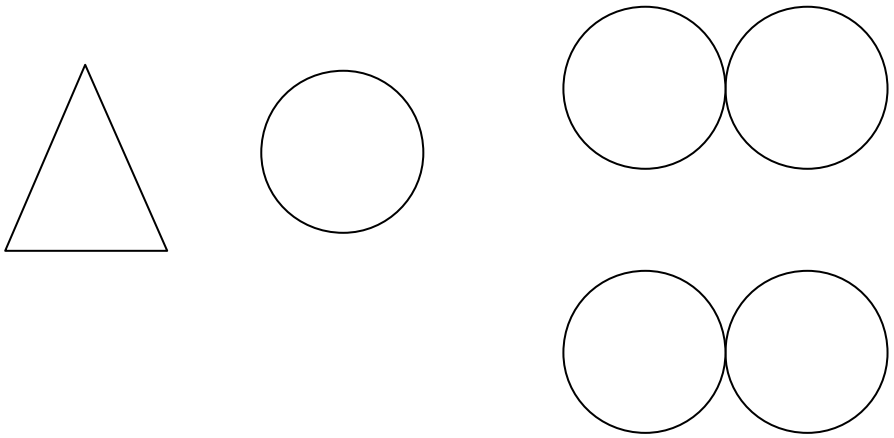

Figure1 Different types of pore shape

Most petroleum reservoirs and many heavily polluted soils are not strongly wetted by water in the presence of oil, even though most of the minerals making up soils and rock are naturally water-wet. During oil migration, oil invades the pore space by a primary drainage process meaning that the system behaves as though it is water-wet. Where oil directly contacts the solid, surface-active components of the oil called asphaltenes adhere to the surface, altering its wettability. Regions of the pore space for which a wetting film of water coats the surface remain water-wet, as do the corners of the pore space where water still resides, and pores that remain completely water-filled. Within a single pore, the surfaces have different wettability, as shown in Fig. 2. This results in a number of different possible fluid configurations during waterflooding, Fig. 3. Most importantly, oil may reside as a layer in the pore space, sandwiched by water in the corner and water the centre Fig. 3f. (Blunt, 1998).

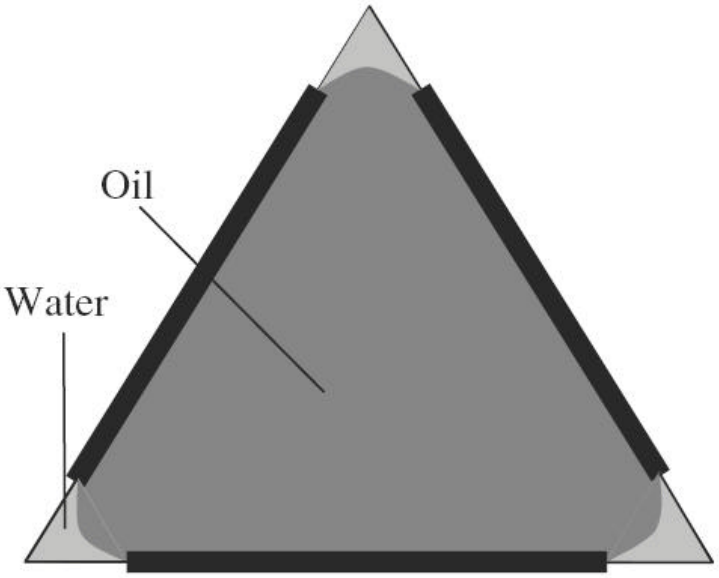

Figure 2 Oil and water in a triangular pore after primary drainage (Blunt, 1998).

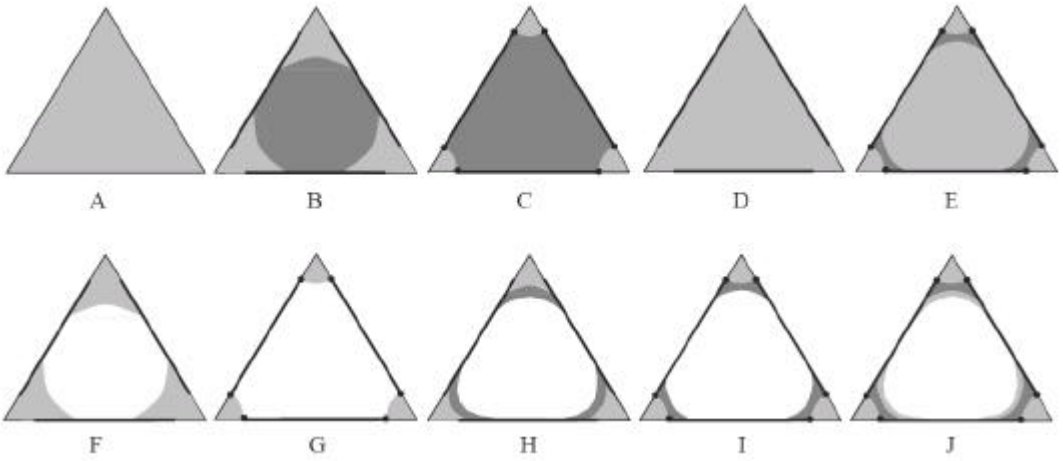

Figure 3 The different pore-scale configurations for waterflooding and gas injection in mixed-wet pores. A bold line indicates regions where the fluid/surface contact is pinned and the contact angle continually varies with capillary pressure. Light grey indicates water, dark grey oil and white is gas (Hui, 2000).

The capillary network modelling concept was first developed by Fatt (1956). Since then, this phenomenon has become a relatively widespread computational modelling approach in the fields of petroleum engineering, chemical engineering and hydrogeology. By distributing the pores and throats on a regular 2D lattice and sequentially filling them in order of inscribed radius using the Young-Laplace equation, he was able to produce capillary pressure and relative permeability curves for drainage (as a function of average saturation) that had the same characteristics as those obtained experimentally.

Further advances in network modelling didn't occur until the late 1970s when computer processing power became more readily available (Valvatne, 2004). Chatzis and Dullien (1977) focused on the assumptions made earlier by Fatt. They observed that 2D networks are not satisfactory to predict the behaviour in 3D. They also noted the importance of coordination number *z* in pore scale networks. Their networks consisted of both pores and throats having assigned volumes.

In the 1980s, percolation theory was used to describe multiphase flow properties is the theoretical foundation for drainage (Koplik and Lasseter, 1985; Wilkinson and Willemsen, 1983; Heiba et al., 1983). Micro-model experiments of drainage and imbibition allowed the pore-scale physics of displacement to be understood. Lenormand *et al*. (1983) used models with rectangular cross-section capillaries to observe and describe the displacement processes in imbibition that still are at the foundations for network modeling – piston-like displacement, snap-off and cooperative pore-body filling.

By the early 1990s interests in pore scale modelling had waned due to the financial problems in the oil industry. But, recently there has been an explosion of interests in pore-scale modelling (Al-Futaisi and Patzek, 2003; Dillard and Blunt, 2000; Dixit et al., 1999; Fenwick and Blunt, 1998; Jackson et al., 2003; Man and Jing, 2000; Okabe and Blunt, 2003). Some advances have been facilitated by increase in computational power. This allows for more comprehensive treatments of displacement processes and more accurate representations of the pore space. As network models continue to improve, their roles are going to be expanded.

CHAPTER 3
THEORY

In pore networks, there are two basic models of multiphase flow such that dynamic and quasi-static. In former case, capillary, gravity and viscous forces in the fluids are taken into account. On the other hand, in the latter case, capillary forces dominate, gravity modifies the magnitude of capillary pressure and the microscopic fluid distributions are frozen at each level of the capillary pressure (Al-Futaisi, 2002). In this study, quasi-static approach is chosen and the viscous forces are ignored. The hydraulic conductance and relative permeabilities of the phases present in the network are then calculated as a result of this model. Moreover, due to its smallness the effect of Buoyancy forces are also ignored. With the developed model, the capillary pressure, saturations and relative permeabilities are calculated during each phase of flooding of oil, water and CO_2.

Firstly, the pores are assumed to be fully saturated with water. Secondly, the capillary pressures for the primary drainage mechanism are calculated. Afterwards the phase areas, and saturations are calculated. Next step is to calculate the conductances for each pore and using these values relative permeabilities for each pore are calculated. This procedure is repeated for both secondary imbibition and CO_2 injection.

There are two network models on which the approach is based on:

- Quasi-static network model: where capillary pressure is imposed on the network and the final static position of fluid-fluid interfaces is determined. Displacement sequence is controlled by invasion capillary pressures.

- Dynamic network model: where a certain inflow rate of one of the fluids is imposed on the network and the subsequent transient pressure response and the associated interface positions are calculated. Displacement decisions are based on pressure difference rules.

3.1 Capillary Entry Pressures in Displacement Mechanisms

The situation of a rock surface when two immiscible fluids contact depends on how well each of the fluids wets the rock. This wetting ability is measured by the contact angle, ?. Drainage occurs when oil or gas displaces water, whereas imbibiton is the case of displacement of water through oil. These two displacement mechanisms have different contact angles such that in drainage receding angle is taken into account and in imbibition case advancing contact angle is used. It is shown in the literature that advancing contact angle is greater than receding contact angle (Valvatne, 2004). The model is simulated as a quasi-static model while calculating the pressures and relative permeabilities.

3.1.1 Primary Drainage Mechanism

In drainage type mechanisms, piston-type displacement is valid. The threshold capillary entry-pressure in drainage in an angular pore is,

$$P^{e}_{c,PD}(q_R) = \frac{s}{r}(1+\sqrt{1-\frac{4G\sum_{i=1}^{n}(E_2^i - E_0^i)}{\cos^2(q_r)}} \tag{3.1}$$

where E_0^i and E_2^i are constants calculated with $q_i = q_r$, and, n is the number of corners in the angular duct, that is n=3 for the triangular cases.

The constants are;

$$E_0^i = \frac{p}{2} - q_i - b_i \tag{3.2}$$

$$E_1^i = \frac{\cos(q_i + b_i)}{\sin(b_i)} \tag{3.3}$$

$$E_2^i = \frac{\cos(q_i + b_i)}{\sin(b_i)}\cos(q_i) \tag{3.4}$$

For a given geometry shape factor (G) is defined simply as the ratio of area to the perimeter squared i.e.,

$$G=A/P^2 \tag{3.5}$$

Thus the shape factor is purely a geometric property of the pore body (Rajiv, 1999).

3.1.2 Secondary Imbibition Mechanism (Piston-Type)

If there is contact angle hysteresis, each Arc Meniscus (AM) hinges about its contact line until the hinging contact angle, $q_{h,i}$, reaches advancing contact angle q_a (Al – Futaisi, 2002).

For a given capillary pressure P_c, the AM $q_{h,i}$ is as follows

$$q_{h,i}(P_c) = \arccos\left[\frac{P_c}{P_c^{\max}}\cos(q_r + b_i)\right] - b_i \tag{3.6}$$

The piston-type displacement in secondary imbibition can be either spontaneous or forced. The difference between spontaneous and forced is that in the former case the capillary pressure is positive whereas in the latter case it occurs at a negative capillary pressure.

The maximum advancing contact angle at which spontaneous secondary imbibition is

$$q_{a,\max} \approx \arccos\left[\frac{-4G\sum_{i=1}^{n}\cos(q_r + b_i)}{\left(\frac{P_c^{\max} r}{s}\right) - \cos(q_r) + 4nG\sin(q_r)}\right] \tag{3.7}$$

where $P_c^{\max}$, is the maximum capillary pressure in primary drainage. The threshold capillary pressure in spontaneous imbibition can be calculated by solving iteratively the following two equations,

$$q_i = \min\left\{q_{h,i}\left(\frac{s}{r_{PT}}\right), q_a\right\} \tag{3.8}$$

$$r_{PT} = \frac{\frac{r^2}{4G} + r_{PT}^2 \sum_{i=1}^{n} (E_0^i - E_2^i)}{2r_{PT} \sum_{i=1}^{n} E_0^i + (\frac{r}{2G} - 2r_{PT} \sum_{i=1}^{n} E_1^i)\cos(q_a)} \tag{3.9}$$

From Eq. 3.8, it is shown that the contact angle is the smallest value of hinging and advancing contact angle. The obtained contact angle is then used in calculation of constants E_0^i , E_1^i and E_2^i which in turn are used to calculate the radius of curvature , r_{PT}, at the capillary entry in Eq. 3.9 (Al – Futaisi, 2002).

Finally, the threshold capillary pressure in piston-type imbibition is calculated from,

$$P_{c,PT}^{e} = \begin{cases} \frac{s}{r_{PT}} & if\ q_a \le q_{a,\max} \\ \frac{2s\cos(q_a)}{r} & if\ q_{a,\max} < q_a < \frac{p}{2} + \min(b_i) \\ -P_{c,PD}^{e}(p - q_a) & if\ q_a \ge \frac{p}{2} + \min(b_i) \end{cases} \tag{3.10}$$

The constants, E_0^i , E_1^i and E_2^i are now calculated with $q_i = p - q_a$

3.1.3 Secondary Imbibition Mechanism (Snap-Off)

Snap-off occurs if two or more of the AMs meet and fuse at a threshold capillary pressure. At this critical pressure, the AMs become unstable and the entire pore fills with water. Snap-off can only occur if there is no Main Terminal Arc Meniscus (MTAM) waiting at the end of the pore (i.e. if piston-type is impossible).

The maximum advancing contact angle at which spontaneous snap-off (positive capillary entry pressure) can occur is,

$$q_{a,\max} = \frac{p}{2} - \min(b_i) \tag{3.11}$$

The radius of curvature of the menisci for each sides of the triangle (i.e. r_{so12}, r_{so13}, and r_{so23}) ought to be calculated for the determination of the snap-off threshold capillary entry-pressure. Below equation is used to find out the radius of curvature of the menisci,

$$r_{soij} = r\frac{\cot(b_i) + \cot(b_j)}{E_1^i + E_1^j} \tag{3.12}$$

It should be noted that, the constants E_1^i and E_1^j are obtained by using the minimum of the hinging angle and the advancing contact angle for corners i and j.

The threshold radius of curvature that causes snap-off in both triangular and square pores is found by the below equation using the radius of curvature of the menisci for each sides of the triangle.

$$r_{so} = \begin{cases} \min(r_{so12}, r_{so23}, r_{so13}) & if \quad n = 3 \\ \dfrac{r}{\cos(q_a) - \sin(q_a)} & if \quad n = 4 \end{cases} \tag{3.13}$$

Finally, the threshold capillary entry-pressure for the snap-off is found by the equation,

$$P_{c,so}^{e} = \begin{cases} \dfrac{s}{r_{so}} & if \;\; q_a < q_{a.\max} \\ P_c^{\max} \dfrac{\cos(q_a + \min(b_i))}{\cos(q_r + \min(b_i))} & if \;\; q_{a,\max} < q_a < p - \min(b_i) \\ P_c^{\max} \dfrac{-1}{\cos(q_r + \min(b_i))} & if q_a \geq p - \min(b_i) \end{cases} \tag{3.14}$$

Note that, in the case of $q_{a,\max} = q_a$ the threshold capillary entry-pressure for snap-off will be zero.

Moreover, the exact flow mechanism (piston-like or snap off) at any stage during imbibition depends on the P_c offered by the two. The event which offers the highest capillary pressure wins (Rajiv, 1999).

3.1.4 CO_2 Injection Mechanism

In CO_2 injection type mechanisms, the displacement procedures are all the same with primary drainage that is the only displacement type is the piston type case (Hui et al., 2000). The threshold capillary entry-pressure in drainage in an angular pore is,

$$P_{c,G}^{e}(q_R) = \frac{s}{r}\left(1+\sqrt{1-\frac{4G\sum_{i=1}^{n}(E_2^i - E_0^i)}{\cos^2(q_r)}}\right) \tag{3.15}$$

where E_0^i and E_2^i are constants calculated with $q_i = q_r$ for the CO_2 case, and, n is the number of corners in the angular duct, that is n=3 for the triangular cases.

The constants are;

$$E_0^i = \frac{p}{2} - q_i - b_i \tag{3.16}$$

$$E_1^i = \frac{\cos(q_i + b_i)}{\sin(b_i)} \tag{3.17}$$

$$E_2^i = \frac{\cos(q_i + b_i)}{\sin(b_i)}\cos(q_i) \tag{3.18}$$

3.2 Phase Areas, Total Areas and Saturations

The determination of areas and saturations of water, oil and gas in each pore is the next step.

The total area of a pore of inscribed radius r is:

$$A_{tot} = r^2 \cot a_i \tag{3.19}$$

where a_i is the corner angle for each vertex of the triangle (Hui et al., 2000).

The area occupied by fluid occupying the corners of a pore, with an interfacial radius of curvature r_{so} is:

$$A_c = r_{soij}^2 [\cos q (\cot a \cos q - \sin q) + q + a - p/2] \tag{3.20}$$

where q is the contact angle and a is the vertex angle.

In the primary drainage case, A_w is the area of water at the corners and found by Eq. 3.20 (q is the advancing contact angle). A_o is the area of oil at the centre and it is the difference between total area and the area of water.

However, in the imbibition case, the corner area is the area of both oil and water at the corners. Therefore, by using Eq.3.20 (q is the receding contact angle), total area of oil and water at the corners are found. If the area of water at the corners found in the primary drainage case is subtracted from the area of oil which is sandwiched can be

found. The area of water in the centre can be found by taking the difference of total area of the pore from the area of oil and water at the corners.

In the gas injection case, CO_2 will be at the centre therefore, at the corners there is oil sandwiched between water phases. Using Eq. 3.20, the area of oil and water phases is found. The area of CO_2 is the difference between the total area and area at the corners.

The saturation of each phase is the sum of the cross-sectional areas of each phase in each pore, divided by the total areas of all the pores.

$$S_w = A_w / A_{tot}$$

$$S_o = A_o / A_{tot}$$

$$S_g = A_g / A_{tot} \tag{3.21}$$

and, $S_w + S_o + S_g = 1$. (3.22)

3.3 Conductances and Flow Rates

For a pore totally full of a single fluid, the following approximation for g based on Poiseuille's law for flow in a circular cylinder is used (Bryant at al., 1993):

$$g = \frac{p\left(\sqrt{A_{tot}/p}\right)^4}{128} \tag{3.23}$$

The above formula is used during the calculation of conductances of the throats.

Primary Drainage: The conductance of oil and water in the primary drainage case is found by,

$$g_o = \frac{p\left(\sqrt{A_o / p}\right)^4}{128} \tag{3.24}$$

and $$g_w = \frac{A_w^2(1-\sin a)^2(f_2 \cos q - f_1)f_3^2}{12n_c \sin^2 a(1-f_3)^2(f_2 + ff_1)^2} \tag{3.25}$$

where:

$$f_1 = p/2 - a - q \tag{3.26}$$

$$f_2 = \cot a \cos q - \sin q \tag{3.27}$$

$$f_3 = \left(\frac{p}{2} - a\right)\tan a \tag{3.28}$$

f is used to indicate the boundary condition at the fluid/fluid interface. In this case f =1 (Zhou et al., 1997).

Secondary Imbibition: The conductances of water in the corners are found by using Eq. 3.25. The conductance of oil layer sandwiched between water phases can be found,

$$g_o = \frac{A_o^3(1-\sin a)^2 \tan a f_3^2}{12n_c A_c \sin^2 a(1-f_3)\left(1 + f_1 f_3 - (1 - f_2 f_3)\sqrt{\frac{A_w}{A_c}}\right)} \tag{3.29}$$

where $f_1 = f_2 = 1$.

The conductance of water at the centre is found by using Eq. 3.23. A_{tot} value in the equation is substituted by A_w at the centre.

With oil layers present, the water conductance has two components – from water in the corners and water in the pore centre. The total conductances are the sum of these two contributions (Hui et al., 2000).

CO_2 Injection: Gas always occupies the centre of the pore space. Thus Eq.3.23 is used for the gas phase conductance with the area of CO_2, A_g, substituted for A_{tot}.

In this case, water occurs both in the corners and layers, as well as an oil layer. The conductance of water in the corners is found by the below equation with f =1,

$$g_{wc} = \frac{A_{wc}^2 (1-\sin a)^2 \left(f_2 \cos q - f_1 - \cot a (1-f_3) r^2\right)^3 f_3^2}{12 n_c \sin^2 a \left(1-f_3^2\right)^2 (f_2 \cos q - f_1)^2 (f_2 + f_1 f_1 - \cot a (1- f_2 f_3) r)^2} \tag{3.30}$$

The sandwiched oil layer conductance is obtained by using Eq.3.29 with $f_1 = f_2 = 1$. Eq. 3.29 is again used to find out the conductance of the water layer by substituting A_o with A_{wl}, A_w with $A_o + A_{wc}$ and $A_c = A_o + A_{wc} + A_{wl}$. The total water conductance is the sum of the conductances of water in the corners and the water layer.

Flow rates: In laminar flow, the volumetric flow rate of fluid I between the two connected nodes I and J is given by,

$$q_{i,IJ} = \frac{g_{i,IJ}}{l_{IJ}} (P_{i,I} - P_{i,J}) \tag{3.31}$$

where l_{IJ} is the spacing between the pore body centres.

$g_{i,IJ}$ is the overall conductances.

The overall conductance, $g_{i,IJ}$ is simply the harmonic mean of conductances of the connecting throat and its two pore bodies;

$$\frac{l_{IJ}}{g_{i,IJ}} = \frac{l_t}{g_{i,t}} + \frac{1}{2}\left(\frac{l_I}{g_{i,I}} + \frac{l_J}{g_{i,J}} \right) \tag{3.32}$$

3.4 Relative Permeability

Relative permeability of water, oil and gas are found by dividing the flow rate of each phase by the total flow rate.

3.5 Adsorption Effect

During the flooding processes there are some concepts which should be taken into account such that adsorption, chemical reactions between phases and solubility effects. In this study, the effects of adsorption in a single pore are analyzed.

Physical adsorption is a major factor governing the behaviour of geothermal reservoirs. That is, adsorbed water on the rock surfaces in a geothermal field has been thought to provide a major source of fluid within the reservoir. In addition to this, the effect of carbon-dioxide flow through water is another main concern for geothermal reservoirs. A single pore model was developed to investigate adsorption considering CO_2 presence in water.

Using this model, adsorption effects with CO_2 presence is discussed at varying temperature and pressure. The model is run at temperatures ranging between 90-130°C at different relative pressures. Stanford experimental adsorption data (Horne et al. 1995) were compared to the results of this developed model. It has been found that, there is a

reasonable fit between the experimental data and the model. A critical pore radius that allows vapour molecule to enter the pore was calculated. It has been observed that the amount of CO_2 adsorbed as well as water in geothermal fields is considerable.

The model is based on three main principles:

- The amount of phase in the pore is known both for the water and the CO_2 – water solution systems since it is assumed that the entire pore is filled with the fluid.

- The system starts by the presence of water .By using Langmuir equations, the amount of adsorption can is calculated. The vapour pressures for the temperatures are gathered from literature.

- The next step is to compute the amount of adsorption due to the CO_2 with presence of water. At this point BET equations are used. The vapour pressure of the solution is computed according to the Raoult's equations.

3.5.1 Bet (Brunauer, Emmett and Teller) Isotherm

The BET theory was first developed by Brunauer et al. (1938) for a flat surface (no curvature) and there is no limit in the number of layers which can be accommodated on the surface. This theory made use of the same assumptions as those used in the Langmuir theory. Let s_0, s_1, s_2 and s_n be the surface areas covered by no layer, one layer, two layer, and n layers of adsorbate molecules, respectively (*Do 1998*).

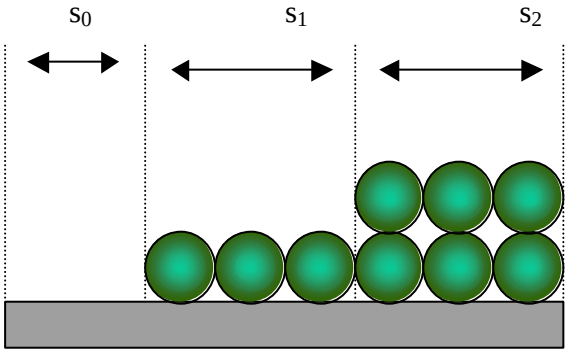

Figure 3.5.1 Schematic Diagram of Multiple layering in BET theory. (*Do, 1998*)

The concept of kinetics of adsorption and desorption proposed by Langmuir is applied to this multiple layering process, that is the rate of adsorption on any layer is equal to the rate of desorption from that layer (*Do 1998*).So, in general:

$$A_i P s_{i-1} = b_i s_i \exp(-E_i / RT) \qquad (3.33)$$

The total area of the solid is the sum of all individual areas, that is:

$$S = ? \; s_i \tag{3.34}$$

The volume of gas adsorbed on the section of the surface having "i" layers is:

$$V_i = V_m \; (i\frac{s_i}{S}) \tag{3.35}$$

Hence, the total volume of gas adsorbed at a given pressure is the sum of all these volumes:

$$V = \frac{V_m}{S} \sum_{i=0}^{\infty} is_i = V_m \frac{\sum_{i=0}^{\infty} is_i}{\sum_{i=0}^{\infty} s_i} \tag{3.36}$$

An expression for s_i in terms of gas pressure is needed in order to obtain the amount of gas adsorbed as a function of pressure. Therefore, a further assumption should be made. That is the ratio of the rate constants of the second and higher layers is equal to each other:

$$\frac{b_2}{a_2} = \frac{b_3}{a_3} = ... = \frac{b_i}{a_i} = g \tag{3.37}$$

According to Langmuir isotherms, it is assumed that the heat of adsorption of the second and subsequent layers are the same and also equal to the heat of liquefaction, E_L:

$$E_2 = E_3 = \ldots\ldots = E_i = E_L \tag{3.38}$$

Therefore, the surface coverage of the section containing I layers of molecules is:

$$s_i = \frac{a_1}{b_1}\, s_0\, g \exp(e1 - e_L)\left[\left(\frac{P}{g}\right) \exp e_L\right] I \tag{3.39}$$

for i = 2, 3…, where e_L is the reduced heat of liquefaction

$$e_L = \frac{E_L}{RT} \tag{3.40}$$

As a result,

$$\frac{V}{V_m} = \frac{Cs_o \sum_{i=1}^{\infty} i\, x_i}{s_o\left(1 + C\sum_{i=1}^{\infty} x_i\right)} \tag{3.41}$$

where the parameter C and the variable x are defined as follows:

$$y = \frac{a_1}{b_1} P \exp(e_1) \tag{3.42}$$

$$x = \frac{P}{g} \exp(e_L) \tag{3.43}$$

$$C = \frac{y}{x} = \frac{a_1 g}{b_1} e^{(e1 - eL)} \tag{3.44}$$

The equation then can be simplified in the following form:

$$\frac{V}{V_m} = \frac{Cx}{(1-x)(1-x+Cx)} \tag{3.45}$$

In order to relate this equation with pressure instead of x, the procedure is as follows:

This model is valid for infinite layers on top of a flat surface. Therefore, the amount adsorbed must be infinity when the gas phase pressure is equal to the vapour pressure, that is $P = P_o$ occurs when $x = 1$. Thus,

$$x = \frac{P}{P_o} \tag{3.46}$$

where $P_o = g. \exp\left(-\frac{E_L}{RT}\right)$ (3.47)

So, the famous BET equation containing two fitting parameters C and V_m becomes:

$$\frac{V}{V_m} = \frac{CP}{(P_o - P)(1+(C-1)(P/P_o))} \tag{3.48}$$

CHAPTER 4
STATEMENT OF THE PROBLEM

In this study, a quasi-static pore-scale network model of two and three-phase flows to compute relative permeabilities, saturation paths and capillary pressures for a variety of displacement processes will be developed. The model will be based on a random network of pores and throats with triangular and circular cross-sections that represent the complex pore space observed in carbonates.

The main goal in this study will be to obtain the effects of different wettabilities of a different-sided triangular pore network in a system which involves CO_2 at the supercritical temperature. Since a significant amount of the world's hydrocarbon reserves are located in carbonate formations the network will be conducted for carbonate cases.

CHAPTER 5
METHOD OF SOLUTION

The following algorithm is used to devlop the pore network simulator:

1) Create the coordinates of the vertices of the triangles in each grid.

2) Calculate each sides, areas and perimeters of the triangles to obtain inscribed radii and interior angles of each triangle.

3) Calculate shape factor of the triangles (Eq. 3.5)

4) Primary Drainage : Refers to the displacement of water by oil.

- Calculate threshold capillary - entry pressures (Eq. 3.1).
- Obtain the flow status of the invaded pores by choosing the minumum of the entry – pressure of neighbour pores.
- Calculate total area of the triangles (Eq. 3.19).
- Calculate the areas of each phase: A_w is the area of water at the corners and found by Eq. 3.20 (q is the advancing contact angle). A_o is the area of oil at the centre and it is the difference between total area and the area of water.
- Create the coordinates of the throats and then obtain the lengths and radii of the throats.
- Calculate the conductances of each phase: Eq. 3.24 and Eq. 3.25 are used to obtain oil and water conductances respectively whereas Eq. 3.23 is used to calculate throat conductance. And Eq. 3.32 is used for overall condcutance of each phase.
- Calculate flow rate (Eq. 3.31) .

- Calculate saturation of each phase (Eq. 3.21).
- Calculate realtive permeability : Obtain by dividing the flow rate of each phase by the total flow rate.
- A mean value for each bin, that is a average saturation of the zone - 5% saturation bin, is then calculated and used in the relative permeability plots

5) *Secondary Imbibition: Refers to the displacement of oil by water.*

- Calculate threshold capillary - entry pressures for piston-like displacement (Eq. 3.10) or snap-off (Eq. 3.14).
- Obtain the flow status of the invaded pores by choosing the maximum of the entry – pressure of neighbour pores.
- Calculate the areas of each phase: Use Eq.3.20 (q is the receding contact angle), to find total area of oil and water at the corners. If the area of water at the corners found in the primary drainage case is subtracted from the area of oil which is sandwiched can be found. The area of water in the centre can be found by taking the difference of total area of the pore from the area of oil and water at the corners.
- Calculate the conductances of each phase: Eq. 3.29 and Eq. 3.23 are used to obtain oil and water conductances respectively whereas Eq. 3.23 is used to calculate throat conductance. And Eq. 3.32 is used for overall condcutance of each phase.
- Calculate flow rate (Eq. 3.31) .
- Calculate saturation of each phase (Eq. 3.21).
- Calculate realtive permeability : Obtain by dividing the flow rate of each phase by the total flow rate.
- A mean value for each bin, that is a average saturation of the zone - 5% saturation bin, is then calculated and used in the relative permeability plots

6) *CO_2 Injection: Refers to the displacement of water by immiscible CO_2.*

- Calculate threshold capillary - entry pressures (Eq. 3.15)
- Obtain the flow status of the invaded pores by choosing the minimum of the entry – pressure of neighbour pores.
- Calculate the areas of each phase: CO_2 will be at the centre therefore, at the corners there is oil sandwiched between water phases. Using Eq. 3.20, the area of oil and water phases is found. The area of CO_2 is the difference between the total area and area at the corners.
- Calculate the conductances of each phase: Eq.3.23 is used for the gas phase conductance with the area of CO_2 , A_g ,substituted for A_{tot}. The sandwiched oil layer conductance is obtained by using Eq.3.29 with $f_1 = f_2 = 1$.Eq. 3.29 is again used to find out the conductance of the water layer by substituting A_o with A_{wl}, A_w with $A_o + A_{wc}$ and $A_c = A_o + A_{wc}+A_{wl}$. The total water conductance is the sum of the conductances of water in the corners and the water layer.
- Calculate flow rate (Eq. 3.31) .
- Calculate saturation of each phase (Eq. 3.21).
- Calculate realtive permeability : Obtain by dividing the flow rate of each phase by the total flow rate.
- A mean value for each bin, that is a average saturation of the zone - 5% saturation bin, is then calculated and used in the relative permeability plots

7) Simulate the code for the displacement processes described with experimental data.

8) Simulate the code for the displacement processes described above with different contact angles.

9) Simulate the code for the miscible CO_2 – water case after primary drainage.

CHAPTER 6
RESULTS AND DISCUSSION

The proposed model is first compared with the experimental results in order to validate the model. The experimental results are taken from mixed-wet intergranular carbonates as reported by Valvatne (2004).In the experimental study, the system was flooded by water as a secondary imbibition case just after the primary drainage is done. After comparing with the experimental data, the effect of contact angles is investigated where in this case immiscible CO_2 is flooded into the system after the secondary imbibition. Finally, the results of the same model are compared with the case of miscible CO_2 flooding.

6.1 Description of the Network

The pores are generated randomly by the model written in Matlab. The pores are assumed to be irregular triangles in order to have a realistic reservoir. That is to say, the coordinates of the vertices of the triangles are determined by the code. The network represents a cube of length 300μ, therefore having a volume of $27* 10^6 \mu^3$. The model is a 2-D network having a grid size of 30 by 30, i.e. 900 pores. There are 1740 throats which are also located randomly to connect the neighbour pores, i.e. the radii and both the lengths and end-coordinates of the throats are varying. The coordination number is fixed as 4 and the cross-sections of the throats are all assumed to be circular in the model. The statistical data of the network is tabulated at Table 6.1.1 and the fluid and rock properties for both immiscible and miscible run can be seen at Table 6.1.2 and 6.1.3 respectively.

The distributions of the inscribed radii are shown in Figure 6.1.1.The pore size distribution in the experiment was assumed to be the pore body to throat radius aspect ratio from the original Berea network since there was no spontaneous displacement data available (Valvatne, 2004).In order to handle with the end effects, the first and the last 10 columns of the model are not used while constructing the relative permeability curves . While calculating relative permeabilities the zones are binned according to the average saturation of the zone, using a 5% saturation bin (increments). A mean value for each bin is then calculated and used in the relative permeability plots (Hughes and Blunt, 2000).

Table 6.1.1: Statistical data of the network

	Pore radius (microns)	**Throat radius (microns)**
Mean	0.7766	0.2022
Standard deviation	0.5563	0.1019
min	0.0014	0.0232
max	2.7789	0.4988

Table 6.1.2: Fluid and Rock Properties Used in Runs of the contact angle effect case

	Case 1	**Case 2**
Temperature (°C)	32	32
Advancing contact angle (deg) in imbibition (Valvatne, 2004)	80	82
Receding contact angle (deg) in drainage (Valvatne, 2004)	25	40
Receding contact angle (deg) in gas injection (Hui, 2000)	40	85
IFT (N/micron) (*Bradley, 1992*)	2.8629e-08	2.8629e-08
Viscosity of oil (N/micron^2/sec) (*Bradley, 1992*)	6.17e-09	6.17e-09
Viscosity of water (N/micron^2/sec) (*Bradley, 1992*)	0.927e-09	0.927e-09
Viscosity of CO_2 (N/micron^2/sec) (*Bradley, 1992*)	0.01522e-03	0.01522e-03

Table 6.1.3: Fluid and Rock Properties Used in Runs of the miscible CO_2 case

	Miscible Case
Temperature (°C)	32
Advancing contact angle (deg) in imbibition (Valvatne, 2004)	80
Receding contact angle (deg) in drainage (Valvatne, 2004)	25
Receding contact angle (deg) in gas injection (Hui, 2000)	40
IFT (N/micron) (*Bradley, 1992*)	2.8629e-08
Viscosity of oil (N/micron^2/sec) (*Bradley, 1992*)	6.17e-09
Viscosity of water (N/micron^2/sec) (*Bradley, 1992*)	0.927e-09
Viscosity of CO_2 (N/micron^2/sec) (*Bradley, 1992*)	0.01522e-03

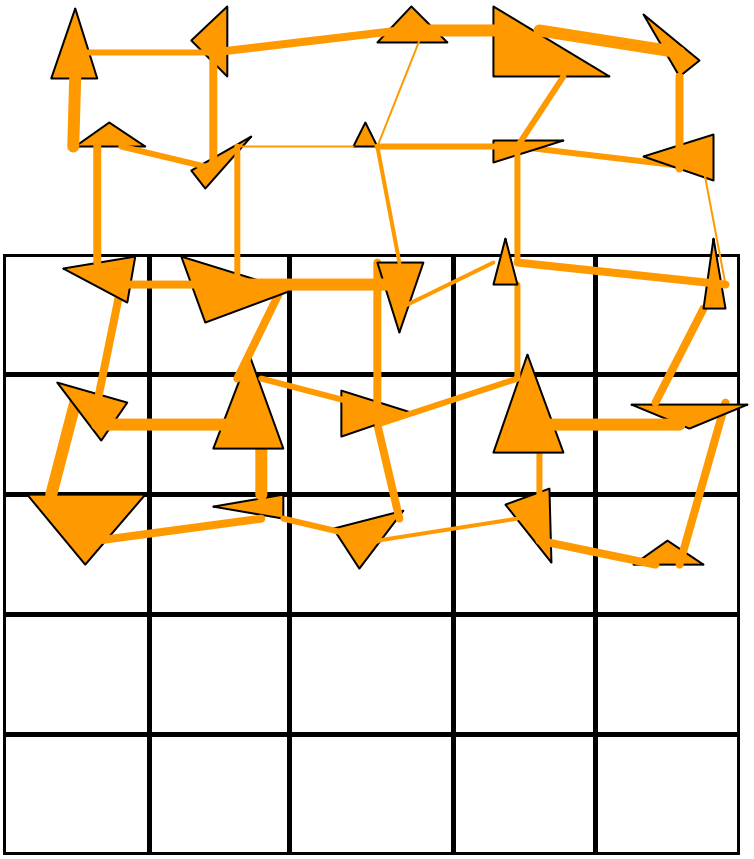

Figure 6.1.1 Sample Network

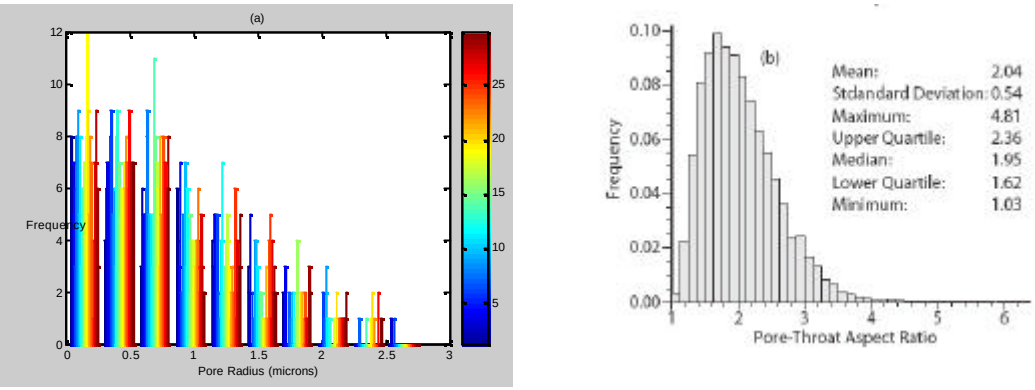

Figure 6.1.2 (a) The distribution of inscribed radii of the model proposed, (b) Distribution of pore to throat radius aspect ratio for original Berea network by Valvatne (2004).

6.2 Comparison of the Model With The Experimental Studies

The relative permeability of the network model was compared to experimental data of intergranular carbonates obtained from literature (Valvatne, 2004).

Table 6.2.1 Fluid and rock properties used in predictions for mixed-wet intergranular carbonates

Surface tension (10^{-9} N/micron) (Valvatne, 2004)	29.9
Water viscosity (10^{-9} N/micron-sec) (Valvatne, 2004)	0.927
Oil viscosity (10^{-9} N/micron-sec) (Valvatne, 2004)	6.17
Oil-wet contact angle (deg) (Valvatne, 2004)	80
Water-wet contact angle(deg) (Valvatne, 2004)	25

The flow path that is predicted during primary drainage is obtained by choosing the minimum entry-threshold pressure where the capillary entry-pressures are calculated with the above fluid and rock properties of mixed-wet intergranular carbonates. Whereas in the secondary imbibition case the flow path that is predicted is obtained by choosing the maximum entry-threshold pressure.

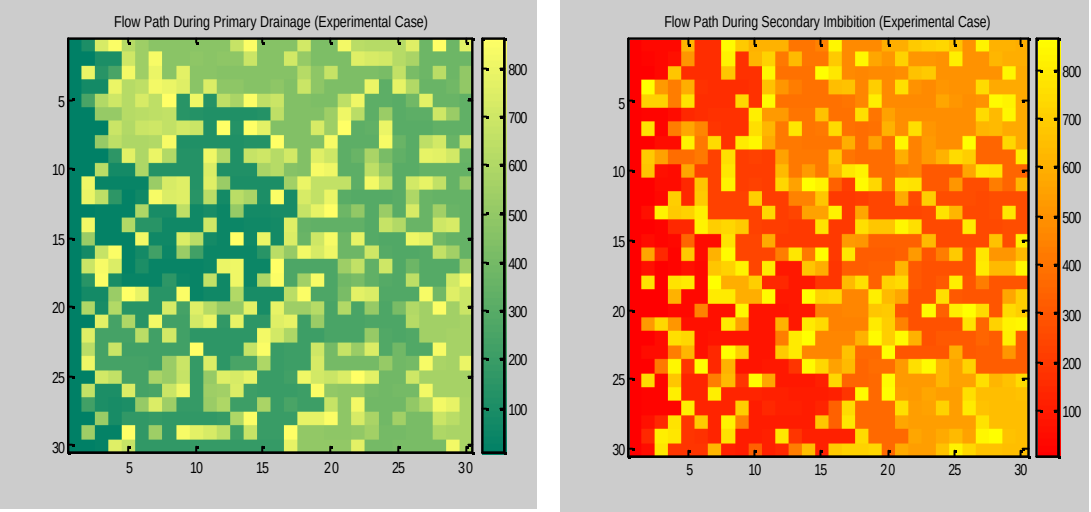

Figure 6.2.1 Flow Path of experimental data run

The colour bars on the right hand side of the figures (Figure 6.2.1) represent the filling sequence of the porous with the invading phase. That is to say #1 is filled before #900.

Relative permeability vs. saturation graph (Figure 6.2.2) data was in good agreement about approximately 44% and 31% error for irreducible oil saturation and water saturation respectively (Table 6.2.2). The errors are due to the differences between the pore size distribution used in the code and in the experiment. Moreover, the contact angle used in the model as an input is assumed to be fixed for the whole network. Valvatne (2004), on the other hand, uses different contact angles for different pores.

Table 6.2.2 Comparison of irreducible fluids

S_{or}		S_{wir}	
exp	pred	exp	pred
0.18	0.125	0.12	0.175

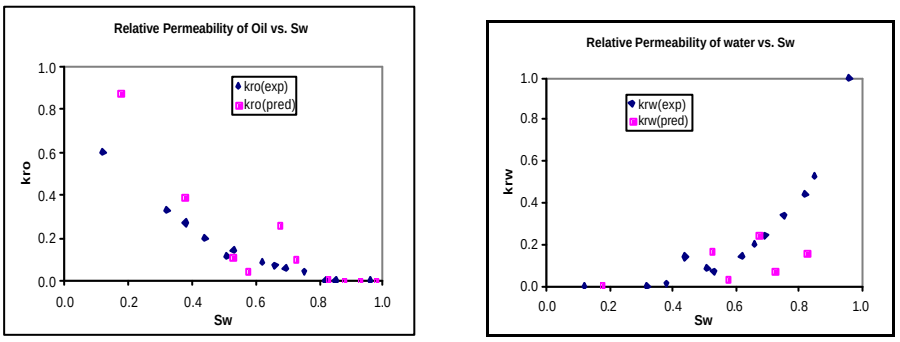

Figure 6.2.2: Experimental (Valvatne, 2004) and model Relative Permeability Vs. Saturation comparison for primary drainage

The results of the proposed pore network in this study is in accord with the results presented by Valvatne (2004) since the flow response is not affected much by the wettability.

As a second step, water is introduced to the system which adds an additional complexity in the wettability characterization. In order to compare the results of the secondary imbibition, water is injected through the proposed model and an error of 31% and 17% are obtained for irreducible water and oil saturation respectively (Table 6.2.3). Thus, it can be accepted as a fairly good agreement. During secondary imbibiton, there is a decrease in errors for irreducible water and oil as seen in Figure 6.2.3.

Table 6.2.3 Comparison of irreducible fluids

S_{or}		S_{wir}	
exp	pred	exp	pred
0.4	0.275	0.27	0.225

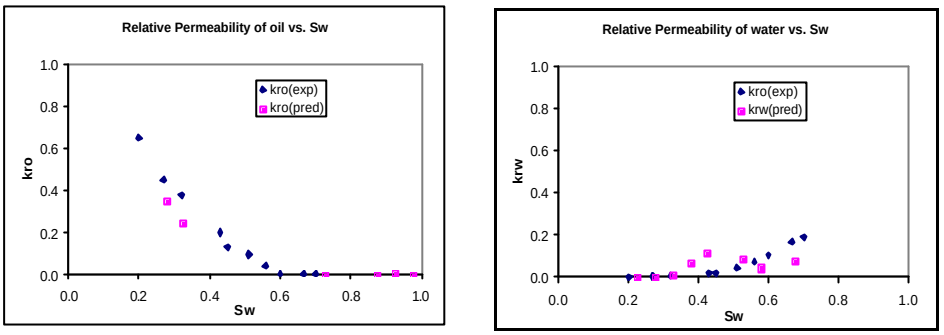

Figure 6.2.3 Experimental (Valvatne, 2004) and model Relative Permeability Vs. Saturation comparison for secondary imbibition.

Although the output of the code, i.e. the relative permeability data, for intergranular carbonates has an error, the constructed network can be considered as representative of the carbonates since the pore size distribution and the values of contact angles in the experimental study are not the same with the proposed model.

The output of the code when immiscible CO_2 is invaded into the system is compared with the data from the literature (Dria et al., 1993). The data from literature (Dria et al., 1993) are the experimental results of CO_2 flooding into a dolomite core (Figure 6.3.4). The temperature and the pore size distribution are different from the network proposed in this study. Therefore, the values of relative permeability are differing (Dria et al., 1993).

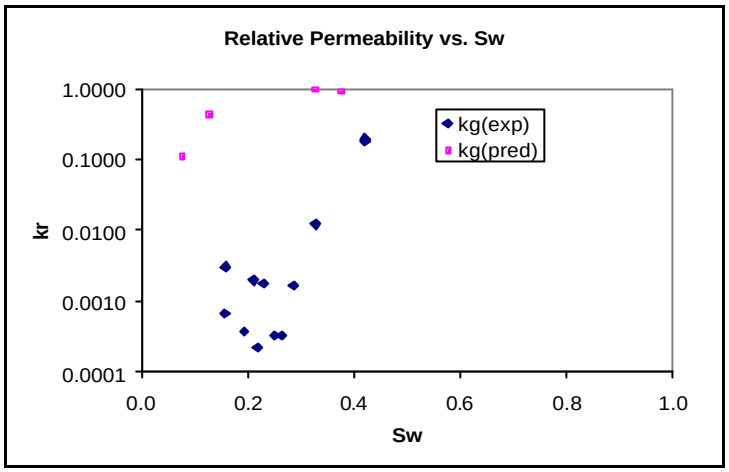

Figure 6.2.4 CO_2 relative permeability data comparison with experiments conducted by Dria et al. (1993) and this study.

6.3 Effects of Contact Angle with Immiscible CO_2 Injection

The network presented is then run for the three-phase flow in which CO_2 injected as the third phase that is introduced to the system at supercritical temperature (32 °C). There is neither experimental nor computational study for the CO_2 injection in three-phase flows above supercritical temperature; therefore the results cannot be compared to any published data. In this section the effects of contact angle at both two phase and three-phase flow is investigated. We have seen that as contact angle is increased in all three flooding processes, the relative permeability data of the fluids had some differences. The results of relative permeability data are tabulated without smoothing.

The colour bars on the right hand side of the figures (Figure 6.3.1) represent the filling sequence of the porous with the invading phase. That is to say #1 is filled before #900.

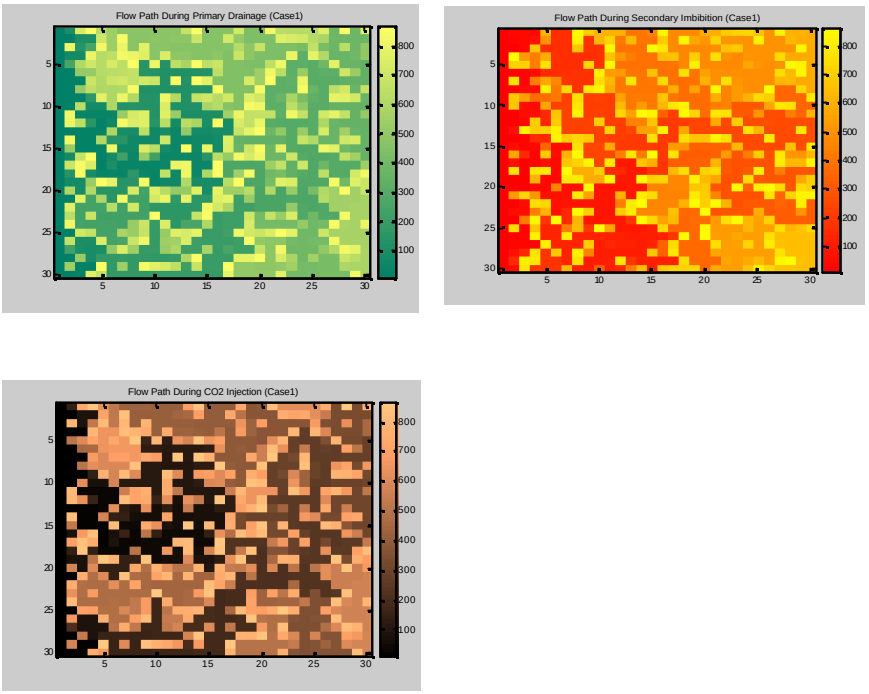

Figure 6.3.1: Flow Path during primary drainage (a), secondary imbibition (b) and CO_2 injection (c)

It can be concluded from the relative permeability Vs. S_w graphs (Figure 6.3.2.a and 6.3.2.b) during primary drainage, when receding contact angle increases (Table 5.1.2), the S_{or} and S_{wir} decreases.

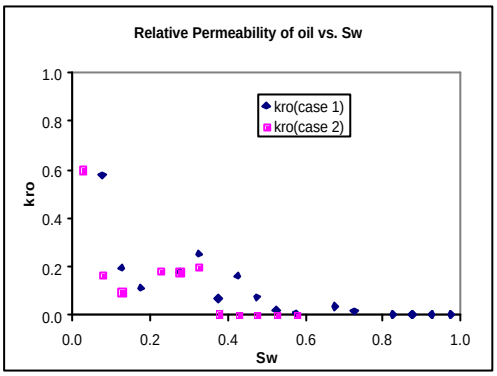

Figure 6.3.2.a: Relative Permeability Vs. Sw during primary drainage for oil cases 1 & 2

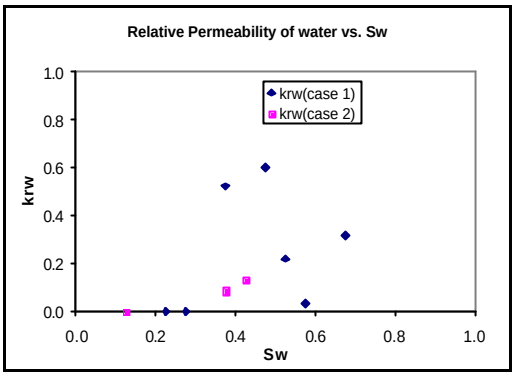

Figure 6.3.2.b: Relative Permeability Vs. Sw during primary drainage drainage for water for cases 1 & 2

The oil gave more response than does the water. That's why the relative permeability of oil is much more scattered (Figure 6.3.3.a, Figure 6.3.3.b).This is due to the fact that oil is more dependent on the saturation history. Whereas relative permeability of water is least scattered indicating that it does not depend on the saturation history. Similar observations are also reported by the studies of Al-Futaisi (2002) and Blunt (1997). Moreover, it is seen that the increase in the advancing angle causes a decrease in residual fluid (oil and water) saturations.

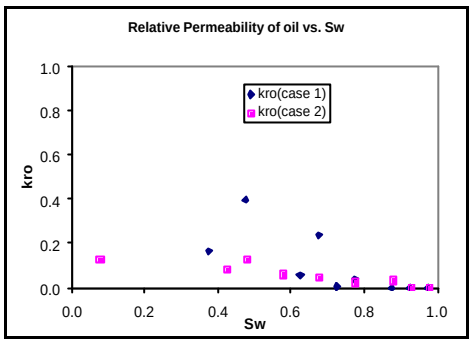

Figure 6.3.3.a: Relative Permeability Vs. Sw during secondary imbibition for oil for cases 1 & 2

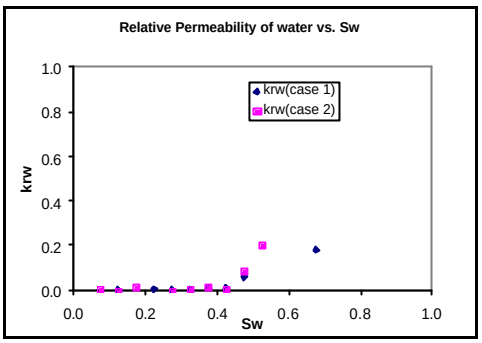

Figure 6.3.3.b: Relative Permeability Vs. Sw during secondary imbibition for water for cases 1& 2

It is found that as the advancing and receding angles in the imbibition and drainage cases respectively increase (Table 5.1.2), the relative permeability of oil decreases when the network is under the supercritical conditions of CO_2. On the other hand, it is observed that relative permeability of water did not change much as the intrinsic angles change. Also, CO_2 decreased slightly ignorable when the intrinsic angles increase (Figure 6.3.4).

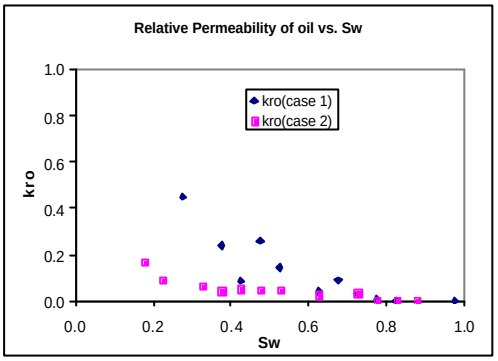

(a)

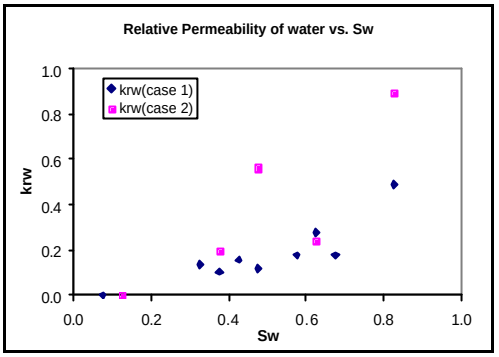

(b)

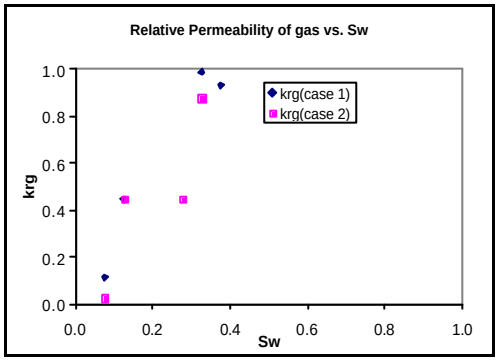

(c)

Figure 6.3.4 Relative Permeability Vs. Sw during CO_2 injection for oil (a); water (b) and gas (c) cases 1 & 2.

6.4 Miscible CO_2 Injection Case

In this section miscible CO_2 in water is introduced to the network after the oil is flooded as a primary drainage process. The effects of the miscibility at the supercritical temperature of CO_2 are examined. In this case, it is assumed that CO_2 is mixed with water at 50% ratio. It is found that, as CO_2 becomes miscible in water the relative permeabilities increase that is the value of relative permeability of water-miscible CO_2 is greater than the values of water obtained in the immiscible case (Figure 6.4.1). Besides, the oil relative permeability values obtained for the immiscible case are smaller than the values obtained in the miscible case. In addition to these, it is observed that the S_{or} value in miscible case is smaller than the immiscible case. On the other hand, S_{wir} in the miscible case is greater than in the immiscible case.

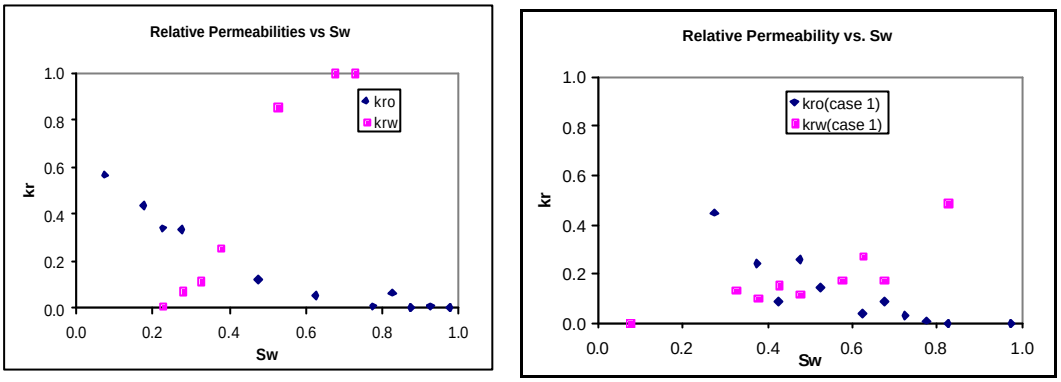

(a) (b)

Figure 6.4.1 Relative Permeability Vs. Sw for the miscible CO_2 case (a), immiscible case (b).

6.5 Comparison Of The Calculated Amount Of Adsorbed Water With The Experimental Data

The effect of adsorption in a pore is studied in this part by using single pore model. The amount of adsorbed water from the literature was compared with the amount of adsorbed water calculated by using Langmuir isotherms. The comparison was made at high pressures and temperatures. This part of the study has stressed adsorption phenomenon to understand the fluid inclusion behaviour and to interpret adsorption properties of water and carbon-dioxide. One of the keys to extracting this information lies in understanding the phase relations of the relevant fluid systems.

Figure 6.5.1 shows the trend of amount of adsorption of water with varying temperatures in a core from The Geysers MLM-3 (Horne et al., 1993) and the relationship between the amount of water adsorbed and relative pressure obtained by the proposed model. It is obviously seen that there is a linear behaviour below relative pressure of 0.6 for both the experimental data and the proposed model. The relative pressure is the ratio of pressure to the reference pressure which in this study is the vapour pressure. While constructing Fig. 6.5.1 Langmuir isotherm equations were used. When the amounts of adsorbed values were compared, a reasonable fit was obtained. There is an error of average 7% when the experimental data is compared with the proposed method up to a relative pressure of 0.6.

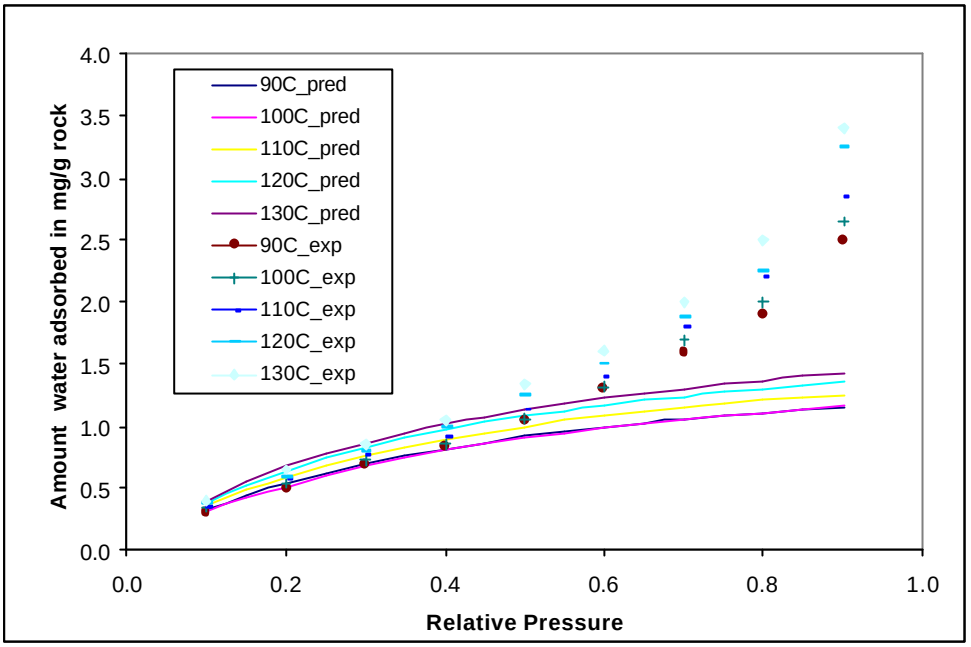

Figure 6.5.1: Adsorption Isotherms on Geysers MLM-3 Sample at Different Temperatures (after Horne et al., 1995) and the data calculated by the proposed model

On the other hand, for relative pressure the values above 0.6, some deviations with respect to the values gathered from experimental data are observed. The error between the computed data and the experimental data becomes significantly more than an average of 25%. When temperature or pressure increases the error becomes higher. This may be due to the fact that Langmuir type isotherms would not give accurate results at high pressures. The Langmuir theory holds for low pressures (Knight et al.). The problem with the Langmuir theory is that at high pressures, there may be more than just monolayer coverage (Knight et al.).

6.6 CO_2-Water Adsorption

The next step is to investigate adsorption of CO_2 with presence of water since aqueous solutions that contain volatile (gas) components are one of the most important types of fluid in the Earth's crust (Diamond 2001). In this study, 5% molar fraction of CO_2 was mixed with water. The secondary adsorption process was investigated in which water was primarily adsorbed. The relative vapour pressure of the mixture was calculated according to this assumption. Later, BET isothermal equations were used in order to calculate the amount of adsorbed values for both CO_2 and water.

The solubility of CO_2 decreases with rising temperature, but increases sharply with rising pressure up to the saturation pressure and a lesser rate thereafter (Spycher et al. 2003). Relatively, the adsorption process of CO_2 has the same trend. Figure 6.6.1 shows the relationship between pressures ranging between approximately 5kPa to 44.5kPa. In this figure, a linear behaviour up to a relative pressure of 0.2 is obtained. But, after that point, as the pressure increases, the amount of CO_2 adsorbed increases .Since adsorption is an exothermic process, the amount of adsorbed CO_2 increases as the temperature increases.

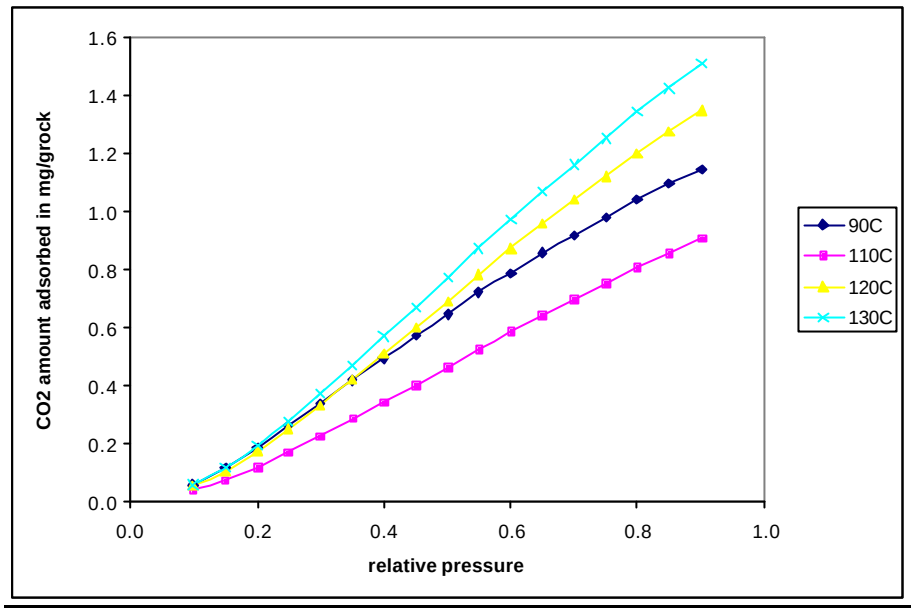

Figure 6.6.1: CO_2 Adsorption isotherms

Figure 6.6.2 shows the comparison of the adsorption tendencies of water and CO_2-water solution at 90°C. It is easily observed that amount of adsorbed water is higher than that of CO_2 at the same temperature and pressure. The major dissimilarity between CO_2 and water arises from the fact that CO_2 is large and non-polar, whereas H_2O is small and dipolar.

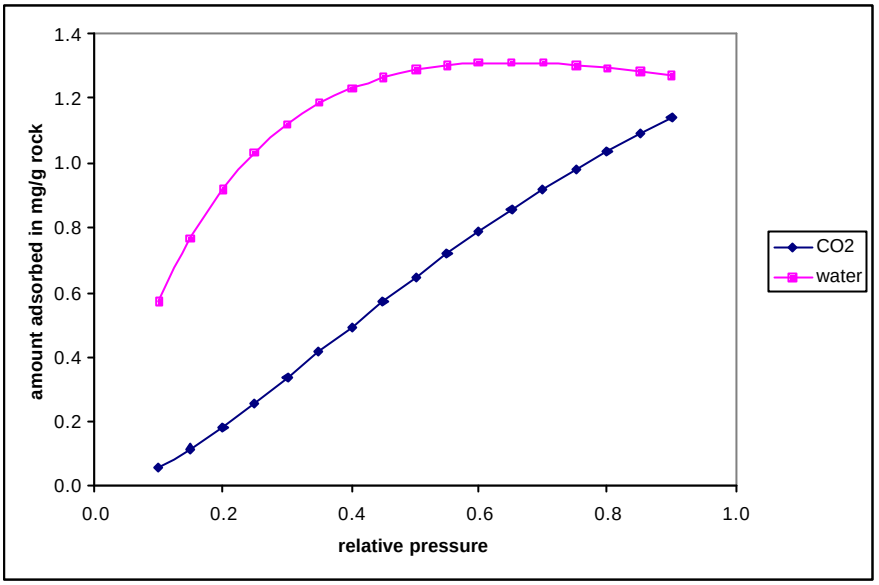

Figure 6.6.2: Comparison of adsorbed amounts at 90°C

Although there are dissimilarities between CO_2 and water in their physical properties, both water and the CO_2-water solution had increasing trends during adsorption processes. Figure 6.6.3 shows the adsorption at 130°C. If the trends both at 90°C and 130 °C are compared, it is observed that at the same pressures, the amount of adsorbed molecule at the secondary adsorption process was more than that of water for the primary adsorption.

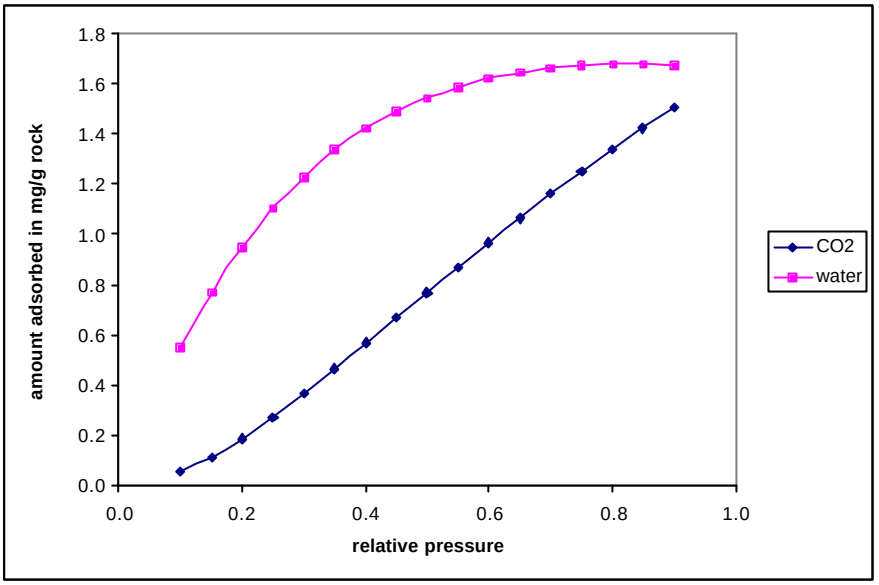

Figure 6.6.3: Comparison of adsorbed amounts at 130°C

The rapid increase of adsorbed molecules in mixture at higher pressures is due to the accuracy of BET equations at higher pressures (*Do, 1998*). This rapid increase is a result of capillary condensation.

Critical radius r_c, which is equivalent to the radius of space extended by a steam molecule, r_g, at a given temperature and pressure is a concern to be discussed in an adsorption process. Critical radius controls the entrance of the vapour molecule. A pore having radius smaller than this value can not be filled with the vapour since capillary condensation cannot take place. Critical radius is obtained as 2.98micrometre.

CHAPTER 7
CONCLUSION

A state of art pore scale network model coded in Matlab is developed in order to represent the real system of reservoir by using irregular triangles as pores, which are located randomly in the grids of the network, and the throats which connect the pores, that are located randomly on the sides of the triangles.

The network is validated with published data. Although the pore size distribution and the assumption that intrinsic angles (advancing and receding angles) are fixed through out the network and are not the same with the experimental study, the proposed model can be accepted as a representative model for mixed-wet carbonates.

It is observed that, during primary oil flooding relative permeability is controlled by the network geometry and the pore-scale displacement. It is also observed that values of relative permeability of oil decreases, whereas relative permeabilities of water increase as the system becomes more like a sandwiched layer.

A single pore model to see the effects of adsorption in a pore is studied. A comparison of the adsorption of water with the literature and an approach which deals mainly the tendency of adsorbed amounts of CO_2-water mixtures towards higher pressures and temperatures is presented. This simple model, taking advantage of Langmuir and BET isotherms, calculates the adsorption of carbon dioxide in water.

It is concluded that water is adsorbed more relative to CO_2. The adsorption behaviour is determined by the ratio of the fluid-wall attractive interaction. For water this ratio is very small, due to the strong hydrogen bonding (H-bonding) between water molecules.

The critical radius that enables vapour molecules enter into the pores is found as 2.98 microns.

RECOMMENDATION

With the outlined methodology a realistic network is aimed to be generated by random pores and throats. The model was simulated by using a fix contact angle although in a real reservoir, pores have different contact angles.

In this study, the miscibility effect of CO_2 was obtained computationally at the supercritical temperature. The results can be compared by conducting experiments at the same conditions such that miscible CO_2- water is injected to a mixed-wet carbonate at supercritical temperature (32 °C).

The adsorption effect which was ignored at the pore network model can be investigated by implementing the developed single pore model into the whole system.

NOMENCLATURE

M	Molecular weight
R	Gas constant, 8.314 J/mol K
T	Temperature
b	Langmuir constant
Q	Heat of adsorption
P_o	Vapour pressure
A	Area of cross section of a node/ throat
A_{eff}	Effective area occupied by non-wetting phase.
A_O	Area of occupied by non-wetting phase.
A_W	Area occupied by the wetting phase
G	Shape factor
g	Fluid conductance
l_{IJ}	Distance between the centres of Ith and Jth nodes.
P	Perimeter of cross-section of a node/ throat
P_c	Capillary pressure
P_c^{MAX}	Maximum capillary pressure
P_{eff}	Effective perimeter of non-wetting phase along the node/ throat cross section.
$q_{i,IJ}$	Volumetric flow rate of ith phase between Ith and Jth nodes.
r	Inscribed radius
r_{soij}	Radius of curvature of the arc menisci.
S_W	Wetting phase saturation

Greek letters

p Spreading pressure

a Corner half angle

?R Receding contact angle

?A Advancing contact angle

?H Hinging contact angle

μ Fluid viscosity

σ? Fluid interfacial tension

Subscripts

A Advancing

eff Effective

H Hinging

i Numeric index for identifying corner angle/ node ID/ throat ID

MAX Maximum

o Oil or non-wetting phase

R Receding

w Water or wetting phase

REFERENCES

Al-Futaisi, Ahmed Mohammed,:" Physically-Based Quasi-Static Pore Network Simulator of Drainage and Imbibition in Two and Three Phase Flow of Immiscible Fluids", Thesis of Doctor of Philosophy, Civil and Environmental Engineering in the Graduate Division of University of California, Berkeley, 2002.

Al-Futaisi, A., and T. W. Patzek,:"Impact of wettability alteration on two-phase flow characteristics of sandstones: A quasi-static description", Water Resources Research, 39, 2003, 1042.

Al-Gharbi, Mohammed, S., Blunt, Martin, J.,:"A 2D dynamic pore network model for modelling primary drainage", 2002.

Bakke, S. and Øren, P.E.: "3-D pore-scale modelling of sandstones and flow simulations in the pore networks," *SPE Journal* 2, No. 2, 1997, p. 136-149.

Bear, J.,: *Dynamics of Fluids in Porous Media*, Dover, Mineola, N.Y., 1972.

Blunt M.J. and King, P.R.,:"Macroscopic Parameters from Simulation of Pore Scale Flow", Phys. Rev. A, 42, 1990, 4780.

Blunt, M.J. and King, P.R. ,:"Relative Permeabilities from Two and Three-Dimensional Pore-Scale Network Modelling", Transport in Porous Media, 6, 1991, 407.

Blunt, M.J., King, M., and Scher, H.: "Simulation and Theory of Two-Phase Flow in Porous Media", Phys. Rev. A, 46, 1992, 7680.

Blunt, M.J. and Scher, H. :"Pore Level Modelling of Wetting", Physical Review E, 52, 1995, 6387.

Blunt, M.J.: "Effects of heterogeneity and wetting on relative permeability using pore level modelling", SPE Journal, 2, March 1997a, 70-87.

Blunt, M.J.: “Pore level modelling of the effects of wettability”, SPE Journal, 2, December 1997b, 494-510.

Blunt, M.J.: “Physically based network modelling of multiphase flow in intermediate-wet media”, Journal of Petroleum Science and Engineering, April 1998.

Bradley,B. : *Petroleum Engineering Handbook* , Society of Petroleum Engineers, Richardson, TX, USA, Third Printing, February 1992.

Brunauer, Stephen, Emmett, Paul Hugh and Teller, Edward,:” Adsorption of Gases in Multimolecular Layers”, Journal of the American Chemical Society. 309, 1938.

Brennan, John, K., Bandosz, Teresa, Thomson, Kendall, T., Gubbins, Keith, E: “Water in porous carbons”, Colloids and Surfaces A: Physicochemical and Engineering Aspects 187-188, 2001, 539-568.

Bryant, S., Blunt, M.J.: “Prediction of Relative Permeability in Simple Porous Media," *Physical review A* 46, August 1992, 2004-2011.

Bryant, S., King, P.R., Mellor D.W.: “Network Model Evaluation of Permeability and Spatial Correlation in a Real Random Sphere Packing," *Transport in Porous Media* 11, 1993, 53-70.

Bryant, S., Cade, C.A., Mellor D.W.: “Permeability Prediction from Geological Models," *AAPG Bulletin* 77, 1993, 1338-1350.

Chatzis, I. and Dullien, F.A.L.: “Modelling pore structures by 2-D and 3-D networks with application to sandstones,” *Journal of Canadian Petroleum Technology* 16, No. 1, 1977, p. 97-108.

Crittenden, Barry and Thomas, W., John, *Adsorption Technology & Design, pp.1-7*, 1998.

Diamond, Larryn, W.,: “Review of the systematics of CO_2-H_2O fluid inclusions”, Lithos55, 2001, pp. 69-99.

Dillard, L. A., and M. J. Blunt, Development of a pore network simulation model to study nonaqueous phase liquid dissolution, Water Resources Research, 36, 2000, 439-454.

Dixit, A.B., McDougall, S.R., and Sorbie, K.S.: “Pore-level investigation of relative permeability hysteresis in water-wet systems,” SPE 37233, Proceedings of the 1997 SPE International Symposium on Oilfield Chemistry, Houston, Feb. 1997.

Dixit, A. B., S. R. McDougall, K. S. Sorbie, and J. S. Buckley, Pore-scale modeling of wettability effects and their influence on oil recovery, SPE Reservoir Evaluation & Engineering, 2, 1999, 25-36.

Do, D., Duong: *Adsorption Analysis: Equilibria and Kinetics* , 1998.

Dria, D.E., Pope, Q.A., Sepehrnoorl, “Three-phase Gas/Oil/Brine/Relative Permeabilities Measured Under CO_2 Flooding Conditions”, SPE Reservoir Engineering, May 1993.

Fatt, I. "The Network Model of Porous Media I. Capillary Pressure Characteristics", Trans. AIME, 207, 1956, 144.

Fenwick, Darryl, H., Blunt, Martin, J.,:”Use of Network Modelling to Predict Saturation Paths, Relative Permeabilities and Oil Recovery for Three Phase Flow in Porous Media”, SPE, 1997.

Fenwick, D. H., and M. J. Blunt, Network modeling of three-phase flow in porous media, SPE Journal 3, 1998, 86-97.

Heiba, A.A, Davis, H.T., and Scriven, L.E.,:"Effect of wettability on two phase relative permeability on two-phase relative permeabilities and capillary pressures", Proceedings of SPE Annual Conference, San Francisco, SPE 12127, 1983.

Hoory, S.E., and Prausnitz, J.M.:"Molecular Thermodynamics of Monolayer Gas Adsorption on Homogeneous and Heterogeneous Solid Surfaces", Chemical Eng. Symposium, vol. 63, 1967.

Horne, N., Roland, Ramey, Jr. Henry, Shang, Shubo, Correa, Antonio and Hornbrook, John,: "Improving Models of Vapour-Dominated Geothermal Fields: The Effects of Adsorption",1995.

Hughes, Richards, G. and Blunt, Martin, J., :" Pore Scale Modeling of Rate Effects in Imbibition", Transport in Porous Media, 40, 2000, 295-322.

Hui, Mun-Hong and Martin J. Blunt,:" Pore-Scale Modelling of Three-Phase Flow and the Effects of Wettability", SPE 59309,2000.

Jackson, M. D., P. H. Valvatne, and M. J. Blunt, Prediction of wettability variation and its impact on flow using pore- to reservoir-scale simulations, Journal of Petroleum Science and Engineering, 39, 2003, 231-246.

Jerauld, G.R. and Salter, S.J.: "Effect of pore-structure on hysteresis in relative permeability and capillary pressure. Pore-level modelling," *Transport in Porous Media* 5, No. 2, 1990, p. 103-151.

Jia ,Liping, "Reservoir Definition Through Integration Of Multiscale Petrophysical Data", Thesis of Doctor of Philosophy, Department of Petroleum Engineering Stanford University, March 2005

Koplik, J. and Lasseter, T.J. "Two-Phase Flow in Random Network Models of Porous Media", SPEJ 22, 1985, 89.

Kovscek, A.R., Wong, H., and Radke, C.J.: “A Pore-Level Scenario for the Development of Mixed Wettability in Oil Reservoirs," *AIChE Journal* 39, No. 6, June 1993, 1072-1085.

Knight, Andrew, Hauser, Rob, Oshier, Joe,: “Gas Adsorption” Chem. 4411L.

Lenormand, R., C. Zarcone, and A. Sarr, “Mechanisms of the Displacement of One Fluid by Another in a Network of Capillary Ducts”, Journal of Fluid Mechanics, 135, 1983, 337-353.

Man, H. N., and X. D. Jing,: “Pore network modelling of electrical resistivity and capillary pressure characteristics”, Transport in Porous Media, 41, 2000, 263-286.

McDougall, S.R., and Sorbie, K.S.: “The impact of wettability on waterflooding: Pore-scale simulation”, SPE Reservoir Engineering. 10, 1995, 208-213.

Nguyen, V.H., Sheppard, A.P., Knackstedt, M.A., Pinczewski, W.V.: “A Dynamic Network Model for Imbibition," paper SPE 90365, presented at 2004 SPE International Petroleum Conference in Mexico held in Puebla, Mexico, 8-9 November 2004.

Okabe, H., and M. J. Blunt, “Pore Space Reconstruction using Multiple-Point Statistics, Journal of Petroleum Science and Engineering”, submitted, 2003.

Oren, P.E., and Pinczewski, W.V.: “Fluid Distribution and Pore-Scale Displacement Mechanisms in Drainage Dominated Three-Phase Flow," Transport in Porous Media, 20, August 1995, 105-133.

Øren, P.E. and Bakke, S.: “Process based reconstruction of sandstones and prediction of transport properties,” Transport in Porous Media, 46, No. 2-3, p. 311-343, 2002.

Rajiv Nand Lulla, :” Pore Scale Modelling Of Flow In 3-D Random Networks” Thesis of Master of Science, Department of Petroleum Engineering Stanford University, Spring 1999.

Spycher, Nicolas, Pruess, Karsten, and Ennis-King, Jonathan,:"CO2-H2O mixtures in the geological sequestration of CO2.I.Assessment and calculation of mutual solubilities from 12 to 100C and up to 600bar", Geochimica et Cosmochimica Acta, Vol 67, No. 16, 2003, pp.3015-3031.

Valvatne, Per Henrik, : *Predictive Pore-Scale Modelling of Multiphase Flow*, Thesis of Doctor of Philosophy, Department of Earth Science and Engineering of Imperial College, London, 2004.

Wilkinson, D. and Williemsen, J.F.: "Invasion Percolation: A New Form of Percolation Theory", J. Phys. A. Math Gen, 16, 1983, 3365-3376.

Zhou, D., Arbabi, S. and Stenby, E.H.: "A Percolation Study of Wettability Effect on the Electrical Properties of Reservoir Rocks," Transport in Porous Media 29, June 1997, 85-98.